Supporting Information

A novel chemical biology and computational approach to expedite the discovery of new-generation polymyxins against life-threatening *Acinetobacter baumannii*

Xukai Jiang[1,2], Nitin A. Patil[2], Mohammad A. K. Azad[2], Hasini Wickremasinghe[2], Heidi Yu[2], Jinxin Zhao[2], Xinru Zhang[2], Mengyao Li[2], Bin Gong[3], Lin Wan[3], Wendong Ma[4], Philip E. Thompson[5], Kai Yang[4], Bing Yuan[4], Falk Schreiber[6,7], Lushan Wang[8], Tony Velkov[9], Kade D. Roberts[2], Jian Li[2*]

[1]National Glycoengineering Research Center, Shandong University, Qingdao, China; [2]Biomedicine Discovery Institute, Infection & Immunity Program, Monash University, Melbourne, Australia; [3]School of Software, Shandong University, Jinan, China; [4]Centre for Soft Condensed Matter Physics and Interdisciplinary Research & School of Physical Science and Technology, Soochow University, Suzhou, China; [5]Medicinal Chemistry, Monash Institute of Pharmaceutical Sciences, Faculty of Pharmacy and Pharmaceutical Sciences, Monash University, Melbourne, Australia; [6]Department of Computer and Information Science, University of Konstanz, Konstanz, Germany; [7]Faculty of Information Technology, Monash University, Melbourne, Australia; [8]State Key Laboratory of Microbial Technology, Shandong University, Qingdao, China; [9]Department of Pharmacology & Therapeutics, University of Melbourne, Melbourne, Australia.

Corresponding author:

*Professor Jian Li. 19 Innovation Walk, Monash University, Clayton campus, Melbourne 3800, Australia. Tel: +61 3 9903 9702; Fax: + 61 3 9905 6450; Email: Jian.Li@monash.edu

This file includes:

Table S1

SI Appendix

Figures S1 to S29

Table S1. Minimum inhibitory concentrations against different *A. baumannii* strains.

Compound	MICs (μg/mL)				
	5075	**ATCC 19606**	**ATCC 17978**	**246-01-C.246**	**248-01-C.248**
PMB_3	0.5	0.25	0.25	0.25	0.25
[Ala^1]-PMB_3	256	512	64	128	256
[Ala^2]-PMB_3	>512	>512	256	>512	>512
[Ala^3]-PMB_3	4	8	4	4	4
[Ala^5]-PMB_3	>512	>512	>512	>512	>512
[Ala^6]-PMB_3	256	256	128	256	128
[Ala^7]-PMB_3	2	1	0.5	0.5	0.5
[Ala^8]-PMB_3	16	16	8	16	16
[Ala^9]-PMB_3	>512	>512	256	256	>512
[Ala^{10}]-PMB_3	1	1	1	1	0.5

SI Appendix

Synthesis of polymyxin B_3 and analogs

Polymyxin B_3:

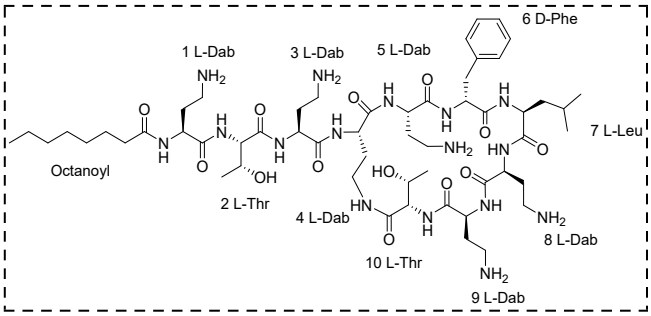

TFA salt was obtained in a yield of 76.6 mg, retention time (t_R) at 214 nm = 12.130 min (HPLC purity: 99.1%). ESI-MS analysis of peak at 12.13 min: *m/z* (monoisotopic) $[M+H]^+$ 1190.20, $[M+2H]^{2+}$ 595.85, $[M+3H]^{3+}$ 397.65. Calculated *m/z* (monoisotopic) for Polymyxin B_3 ($C_{55}H_{96}N_{16}O_{13}$) $[M+H]^+$ 1189.7, $[M+2H]^{2+}$ 595.37, $[M+3H]^{3+}$ 397.24.

[Ala^1]-Polymyxin B_3:

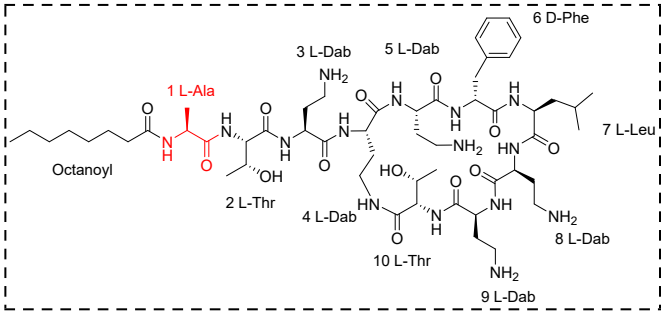

TFA salt was obtained in a yield of 60.5 mg, retention time (t_R) at 214 nm = 12.693 min (purity: 99.1%). ESI-MS analysis of peak at 12.69 min: *m/z* (monoisotopic) $[M+H]^+$ 1161.20, $[M+2H]^{2+}$ 581.45, $[M+3H]^{3+}$ 388.05. Calculated *m/z* (monoisotopic) for [Ala^1]-Polymyxin B_3 ($C_{54}H_{93}N_{15}O_{13}$) $[M+H]^+$ 1160.71, $[M+2H]^{2+}$ 580.85, $[M+3H]^{3+}$ 387.57.

[Ala^2]-Polymyxin B_3:

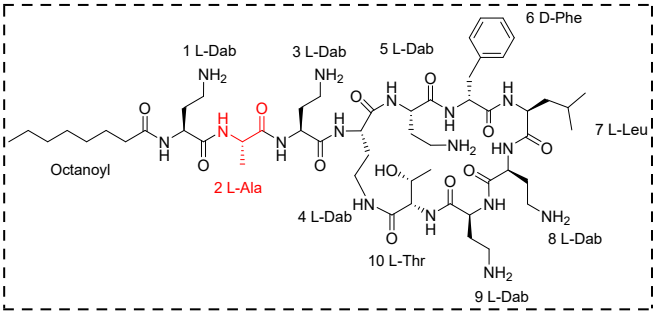

TFA salt was obtained in a yield of 84.6 mg, retention time (t_R) at 214 nm = 12.065 min (HPLC purity: 99.1%). ESI-MS analysis of peak at 12.07 min: *m/z* (monoisotopic) $[M+H]^+$ 1160.20,

$[M+2H]^{2+}$ 580.90, $[M+3H]^{3+}$ 387.70. Calculated *m/z* (monoisotopic) for [Ala^2]-Polymyxin B_3 ($C_{54}H_{94}N_{16}O_{12}$) $[M+H]^+$ 1159.72, $[M+2H]^{2+}$ 580.36, $[M+3H]^{3+}$ 387.24.

[Ala^3]-Polymyxin B_3:

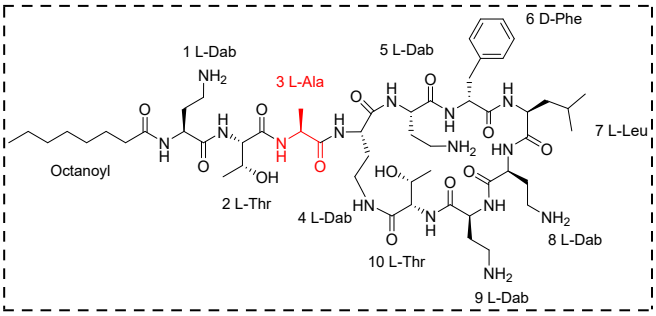

TFA salt was obtained in a yield of 68.2 mg, retention time (t_R) at 214 nm = 12.408 min (HPLC purity: 98.7%). ESI-MS analysis of peak at 12.408 min: *m/z* (monoisotopic) $[M+H]^+$ 1161.20, $[M+2H]^{2+}$ 581.40, $[M+3H]^{3+}$ 388.05. Calculated *m/z* (monoisotopic) for [Ala^3]-Polymyxin B_3 ($C_{54}H_{93}N_{15}O_{13}$) $[M+H]^+$ 1160.71, $[M+2H]^{2+}$ 580.85, $[M+3H]^{3+}$ 387.57.

[Ala^5]-Polymyxin B_3:

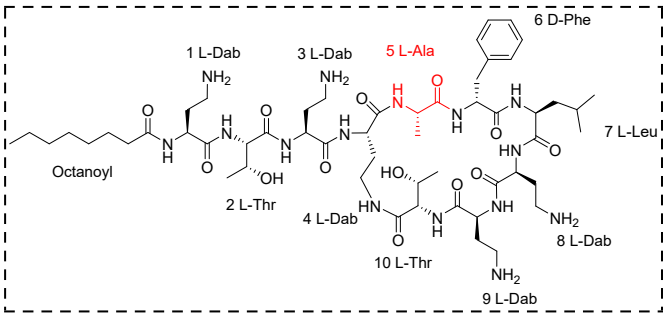

TFA salt was obtained in a yield of 49.0 mg, retention time (t_R) at 214 nm = 12.571 min (HPLC purity: 98.9%). ESI-MS analysis of peak at 12.571 min: *m/z* (monoisotopic) $[M+H]^+$ 1161.20, $[M+2H]^{2+}$ 581.45, $[M+3H]^{3+}$ 388.05. Calculated *m/z* (monoisotopic) for [Ala^5]-Polymyxin B_3 ($C_{54}H_{93}N_{15}O_{13}$) $[M+H]^+$ 1160.71, $[M+2H]^{2+}$ 580.85, $[M+3H]^{3+}$ 387.57.

[Ala^6]-Polymyxin B_3:

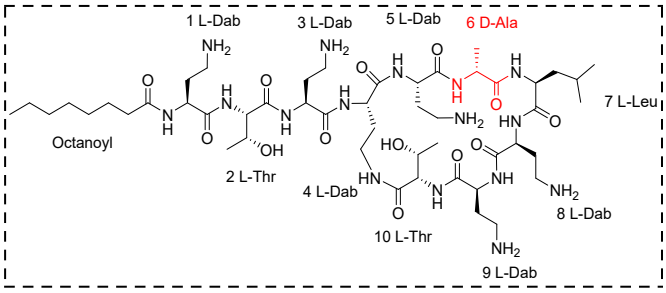

TFA salt was obtained in a yield of 36.8 mg, retention time (t_R) at 214 nm = 11.238 min (HPLC purity: 98.0%). ESI-MS analysis of peak at 11.238 min: *m/z* (monoisotopic) $[M+H]^+$ 1114.20, $[M+2H]^{2+}$ 557.90, $[M+3H]^{3+}$ 372.35. Calculated *m/z*

(monoisotopic) for [Ala^6]-Polymyxin B_3 ($C_{49}H_{92}N_{16}O_{13}$) $[M+H]^+$ 1113.70, $[M+2H]^{2+}$ 557.35, $[M+3H]^{3+}$ 371.90.

[Ala^7]-Polymyxin B_3:

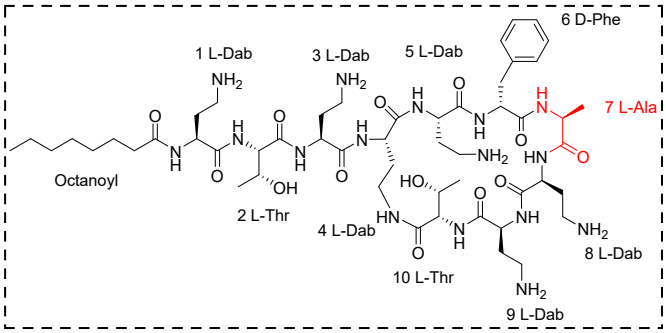

TFA salt was obtained in a yield of 41.0 mg, retention time (t_R) at 214 nm = 11.391 min (HPLC purity: 98.0%). ESI-MS analysis of peak at 11.391 min: *m/z* (monoisotopic) $[M+H]^+$ 1148.20, $[M+2H]^{2+}$ 574.90, $[M+3H]^{3+}$ 383.70. Calculated *m/z* (monoisotopic) for [Ala^7]-Polymyxin B_3 ($C_{52}H_{90}N_{16}O_{13}$) $[M+H]^+$ 1147.69, $[M+2H]^{2+}$ 574.34, $[M+3H]^{3+}$ 383.23.

[Ala^8]-Polymyxin B_3:

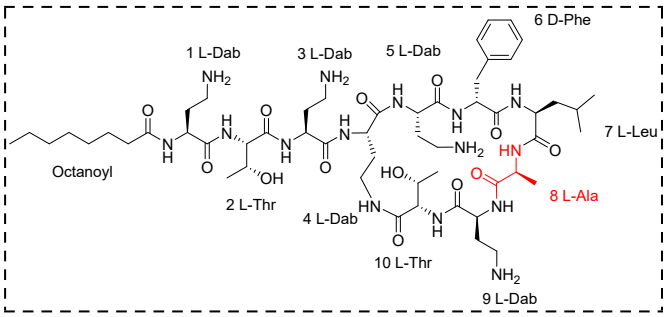

TFA salt was obtained in a yield of 45.0 mg, retention time (t_R) at 214 nm = 12.398 min (HPLC purity: 97.7%). ESI-MS analysis of peak at 12.398 min: *m/z* (monoisotopic) $[M+H]^+$ 1161.20, $[M+2H]^{2+}$ 581.40, $[M+3H]^{3+}$ 388.05. Calculated *m/z* (monoisotopic) for [Ala^8]-Polymyxin B_3 ($C_{54}H_{93}N_{15}O_{13}$) $[M+H]^+$ 1160.71, $[M+2H]^{2+}$ 580.85, $[M+3H]^{3+}$ 387.57.

[Ala^9]-Polymyxin B_3:

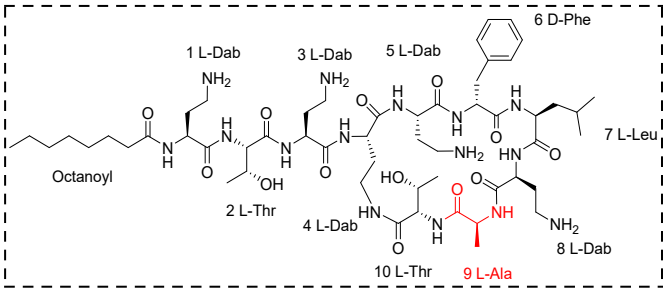

TFA salt was obtained in a yield of 65.3 mg, retention time (t_R) at 214 nm = 12.638 min (HPLC purity: 98.8%). ESI-MS analysis of peak at 12.638 min: *m/z* (monoisotopic) $[M+H]^+$ 1161.20, $[M+2H]^{2+}$ 581.45, $[M+3H]^{3+}$ 388.05. Calculated *m/z*

(monoisotopic) for [Ala^{9}]-Polymyxin B_3 ($C_{54}H_{93}N_{15}O_{13}$) $[M+H]^+$ 1160.71, $[M+2H]^{2+}$ 580.85, $[M+3H]^{3+}$ 387.57.

[Ala$_{10}$]-Polymyxin B$_3$:

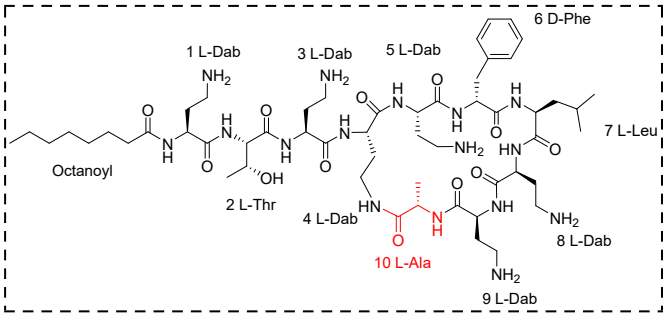

TFA salt was obtained in a yield of 51.3 mg, retention time (t_R) at 214 nm = 12.167 min (HPLC purity: 98.8%). ESI-MS analysis of peak at 12.167 min: *m/z* (monoisotopic) $[M+H]^+$ 1160.15, $[M+2H]^{2+}$ 580.95, $[M+3H]^{3+}$ 387.70. Calculated *m/z* (monoisotopic) for [Ala^{10}]-Polymyxin B_3 ($C_{54}H_{94}N_{16}O_{12}$) $[M+H]^+$ 1159.72, $[M+2H]^{2+}$ 580.36, $[M+3H]^{3+}$ 387.24.

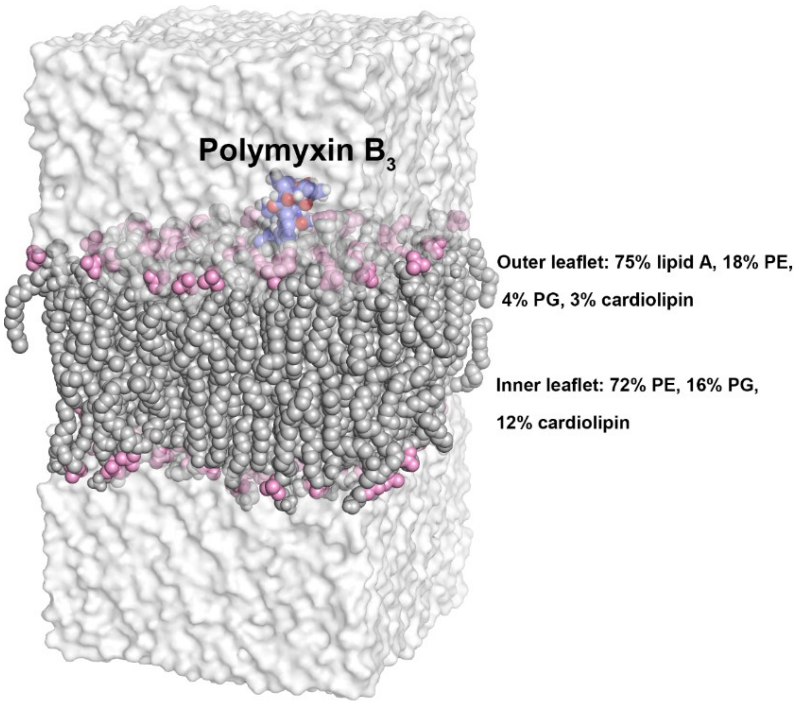

Figure S1. The equilibrated simulation box. Water shell is shown in transparent surface model, the polymyxin molecule is displayed as blue spheres, and the bacterial outer membrane is shown in gray spheres with pink phosphate groups. The lipid composition of the outer membrane is shown for each membrane leaflet. PE, phosphatidylethanolamine; PG, phosphatidylglycerol.

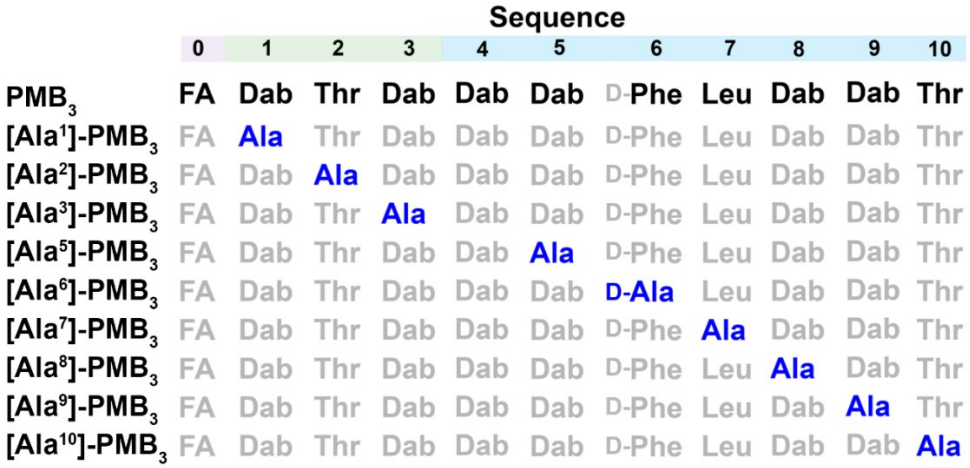

Figure S2. Library of alanine-substituted polymyxin B_3 analogs. FA: octanoyl; Dab: L-α-γ-diaminobutyric acid; Thr: threonine; Phe: phenylalanine; Leu: Leucine.

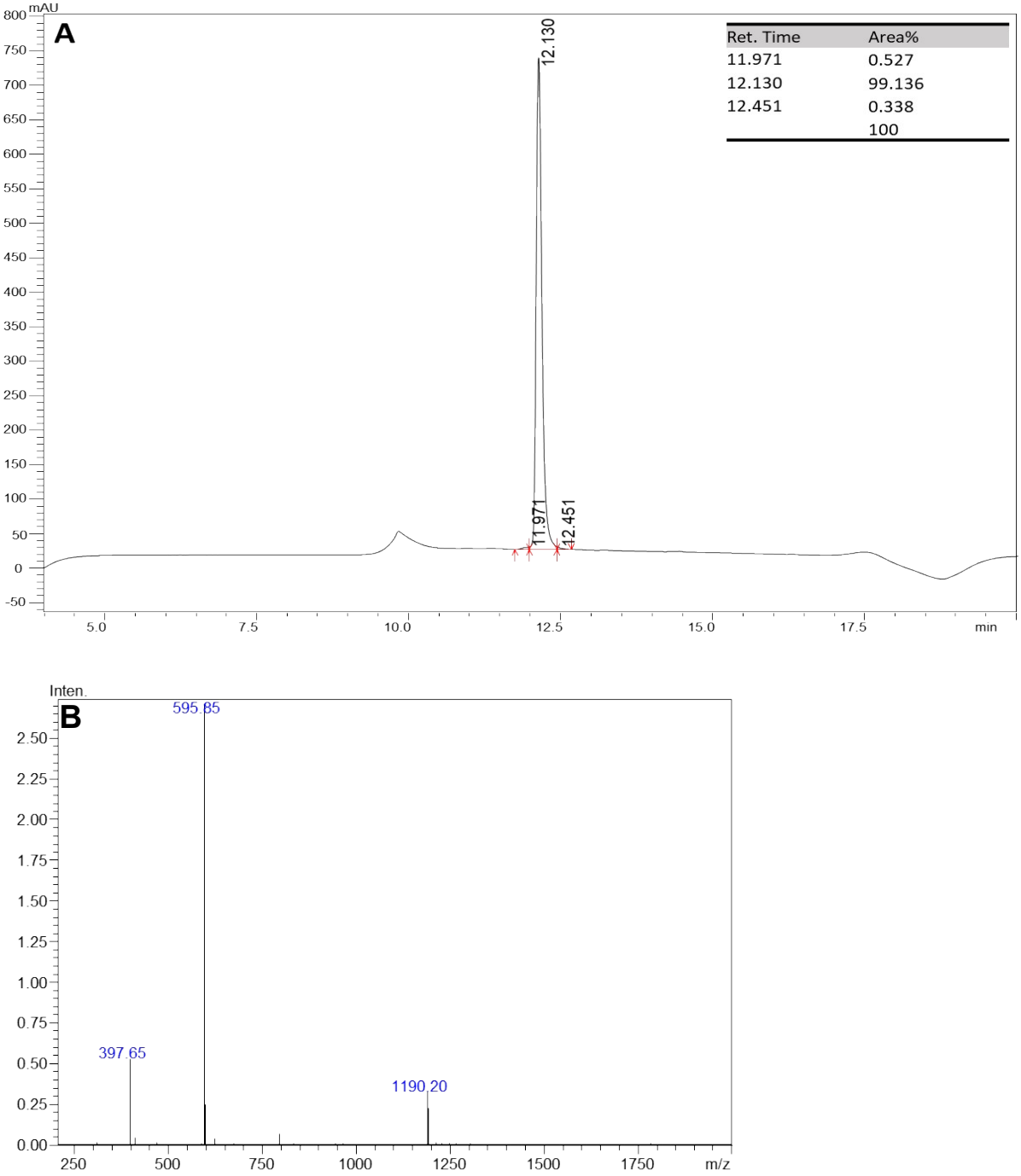

Figure S3. LC-MS profile for polymyxin B_3. (**A**) LC profile at 214 nm. (**B**) MS spectrum of the peak at 12.130 min.

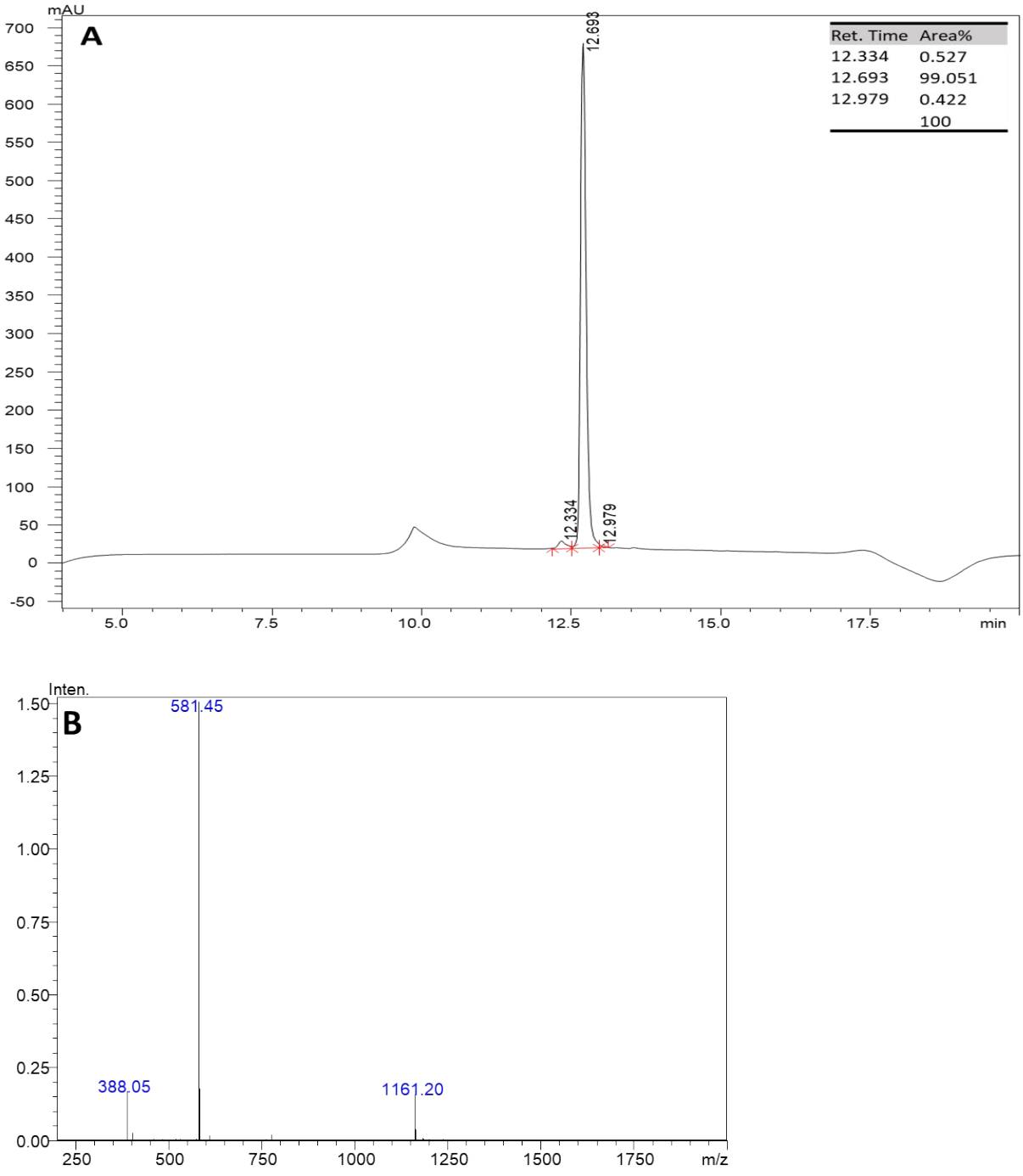

Figure S4. LC-MS profile for [Ala^1]-Polymyxin B$_3$. (**A**) LC profile at 214 nm. (**B**) MS spectrum of the peak at 12.693 min.

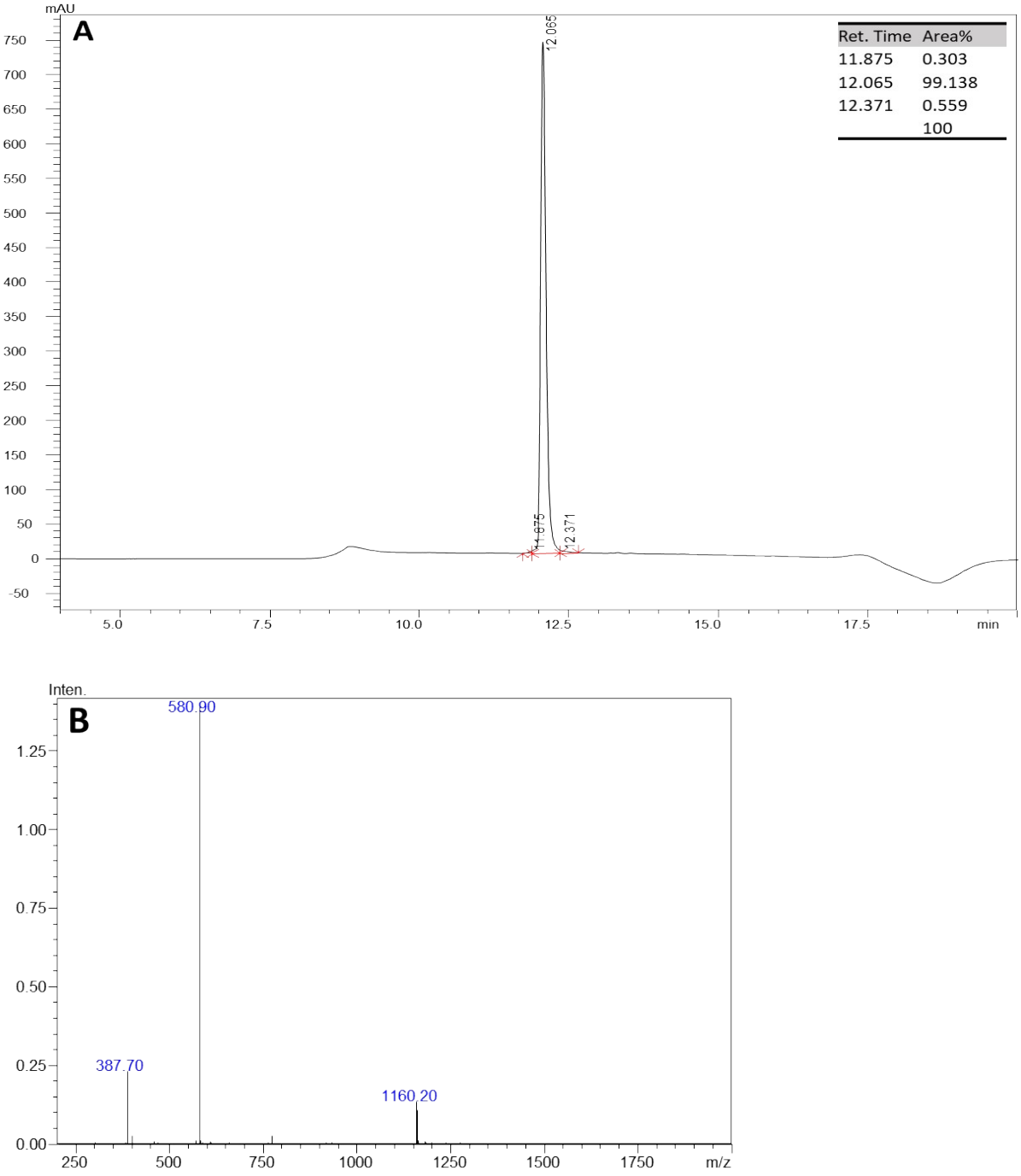

Figure S5. LC-MS profile for [Ala^2]-Polymyxin B$_3$. (**A**) LC profile at 214 nm. (**B**) MS spectrum of the peak at 12.065 min.

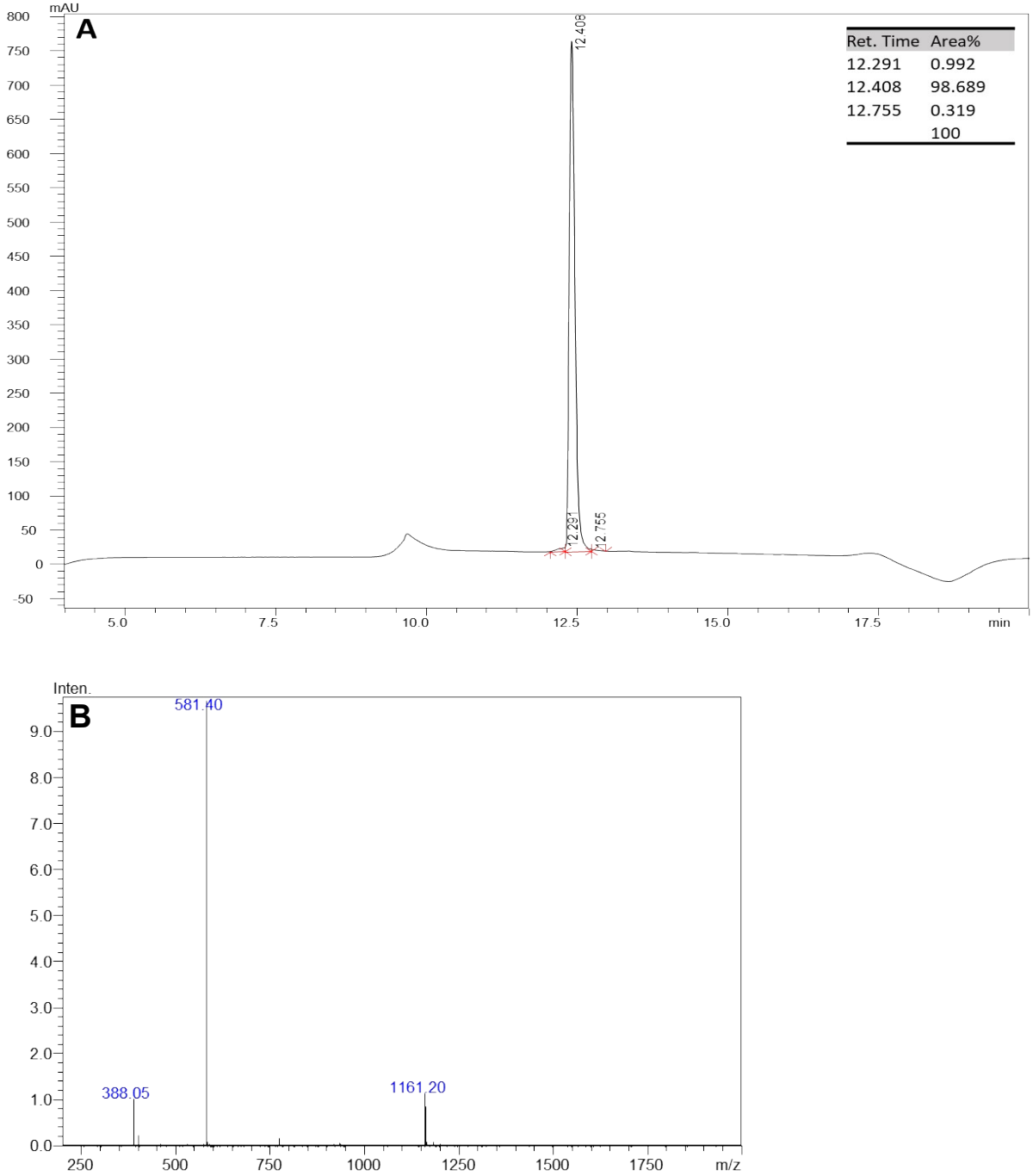

Figure S6. LC-MS profile for [Ala^3]-Polymyxin B$_3$. (**A**) LC profile at 214 nm. (**B**) MS spectrum of the peak at 12.408 min.

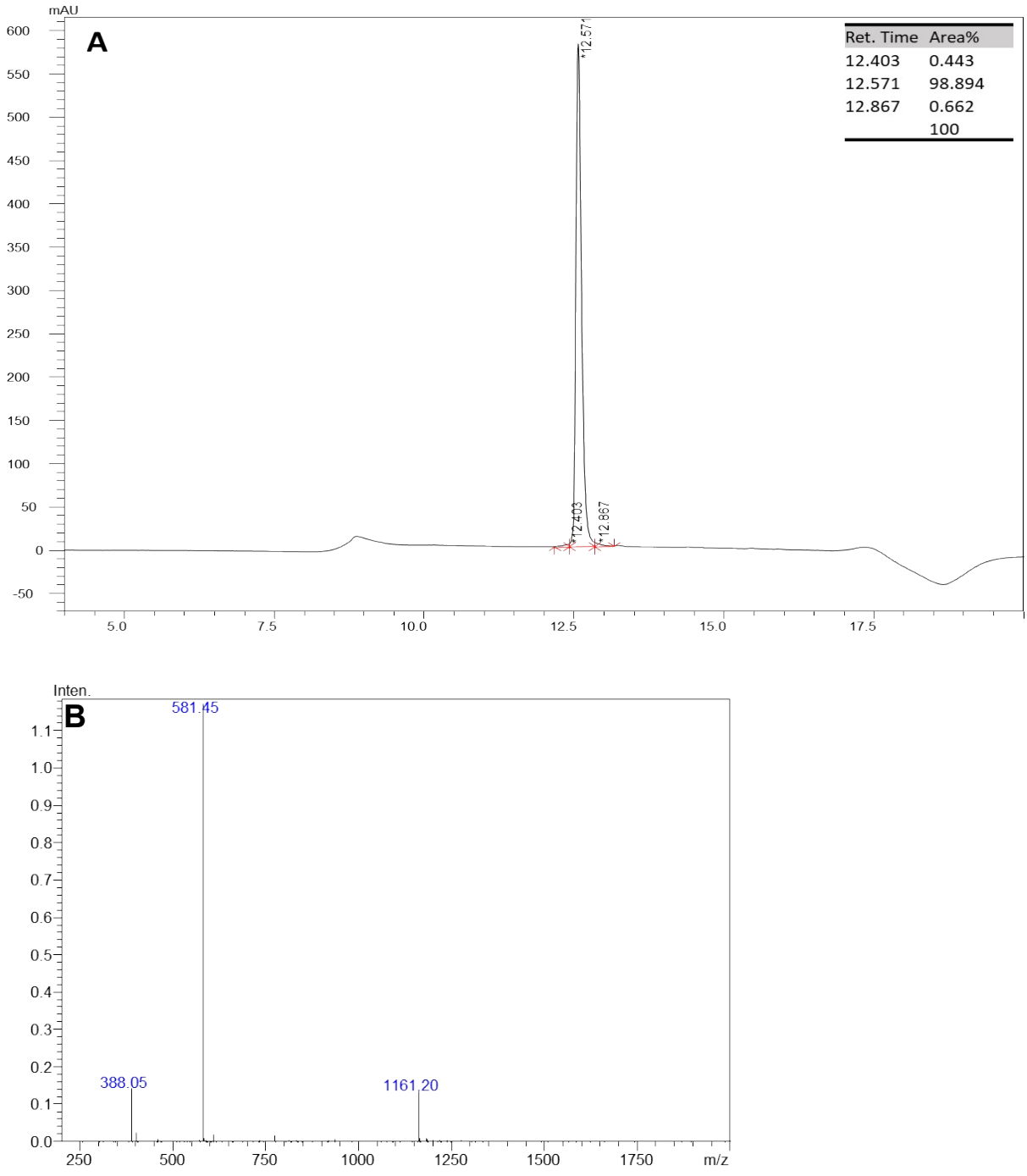

Figure S7. LC-MS profile for [Ala^5]-Polymyxin B$_3$. (**A**) LC profile at 214 nm. (**B**) MS spectrum of the peak at 12.571 min.

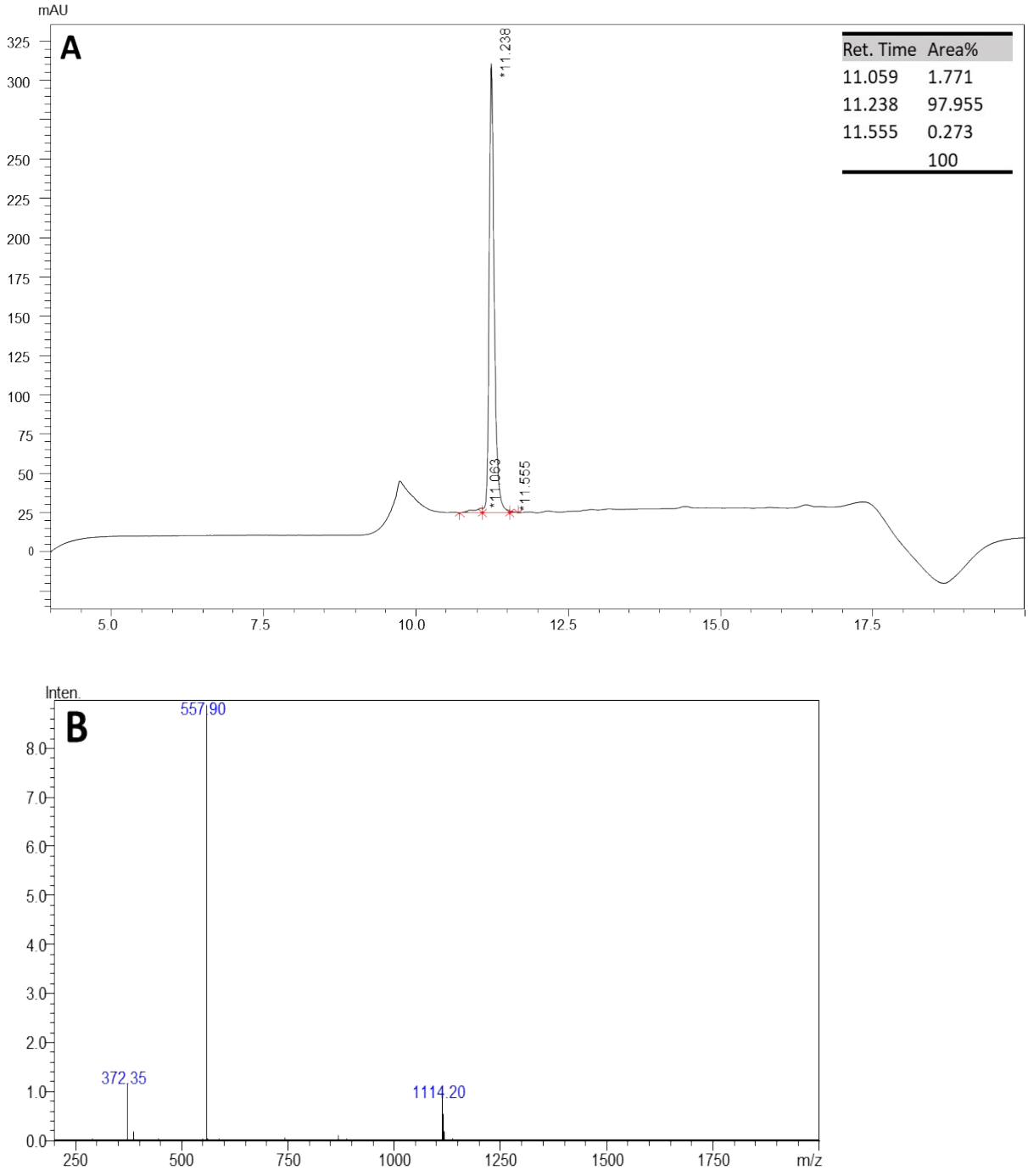

Figure S8. LC-MS profile for [Ala^6]-Polymyxin B$_3$. (**A**) LC profile at 214 nm. (**B**) MS spectrum of the peak at 11.238 min.

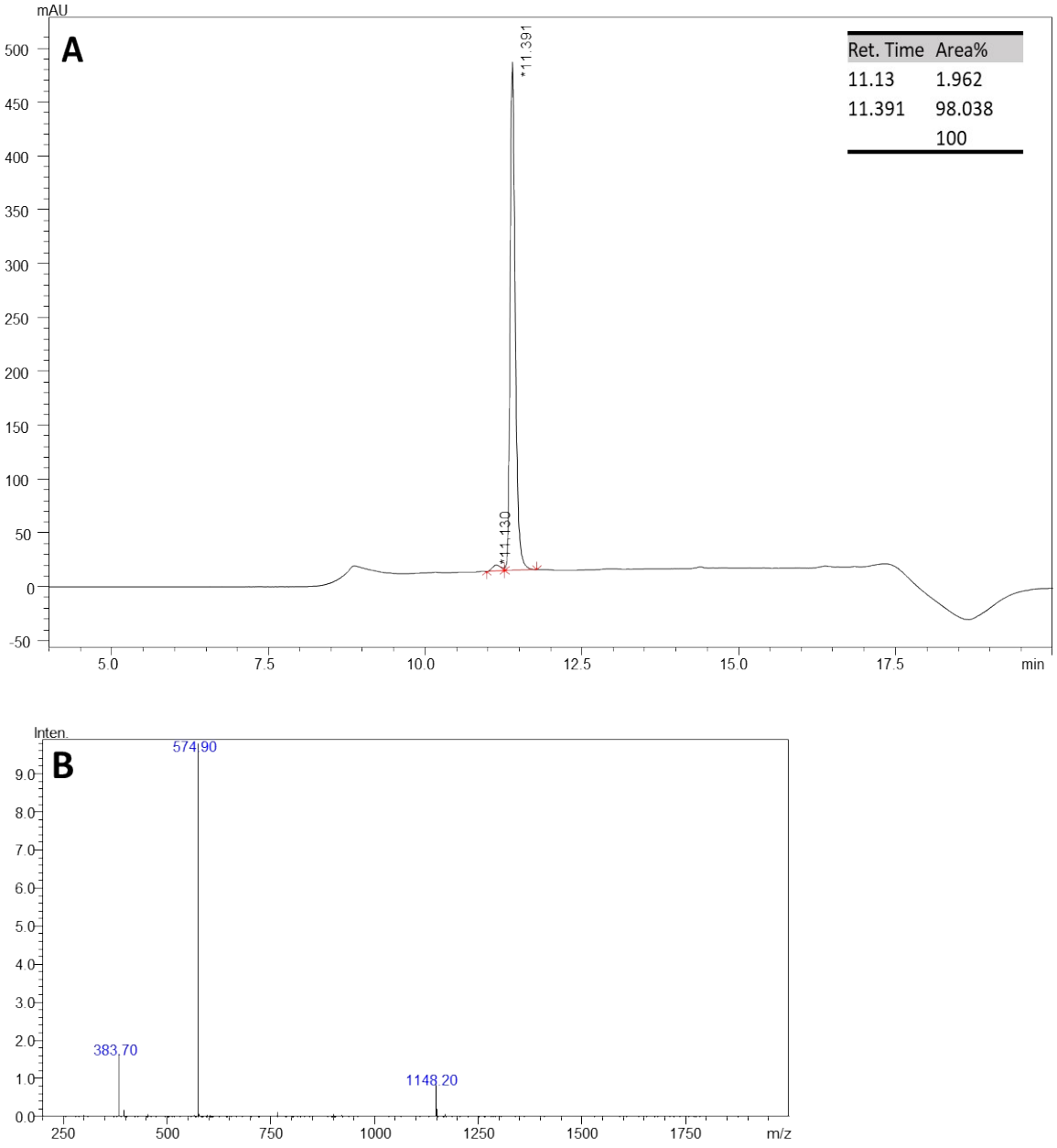

Figure S9. LC-MS profile for [Ala^7]-Polymyxin B$_3$. (**A**) LC profile at 214 nm. (**B**) MS spectrum of the peak at 11.391 min.

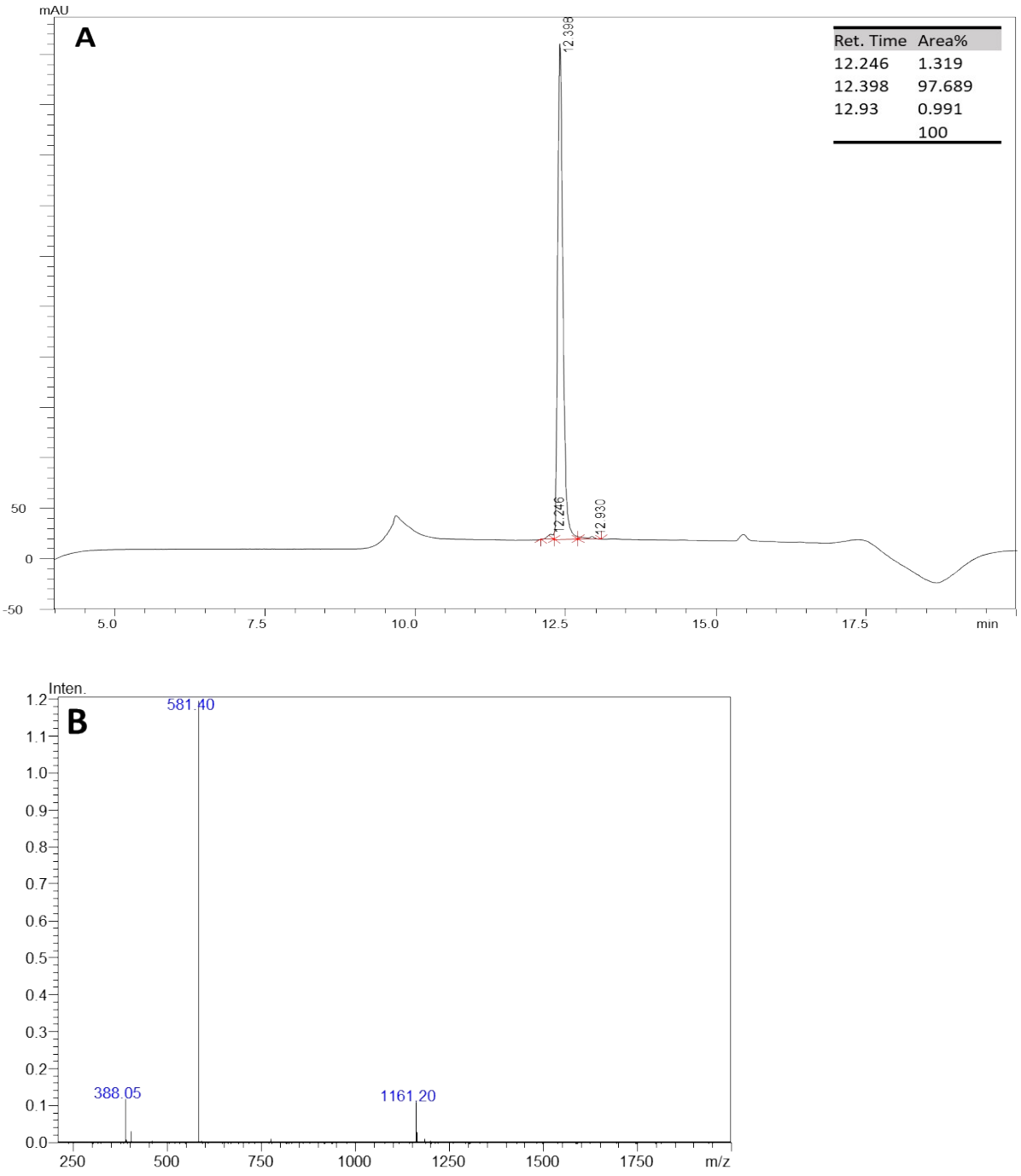

Figure S10. LC-MS profile for [Ala^{8}]-Polymyxin B$_{3}$. (**A**) LC profile at 214 nm. (**B**) MS spectrum of the peak at 12.398 min.

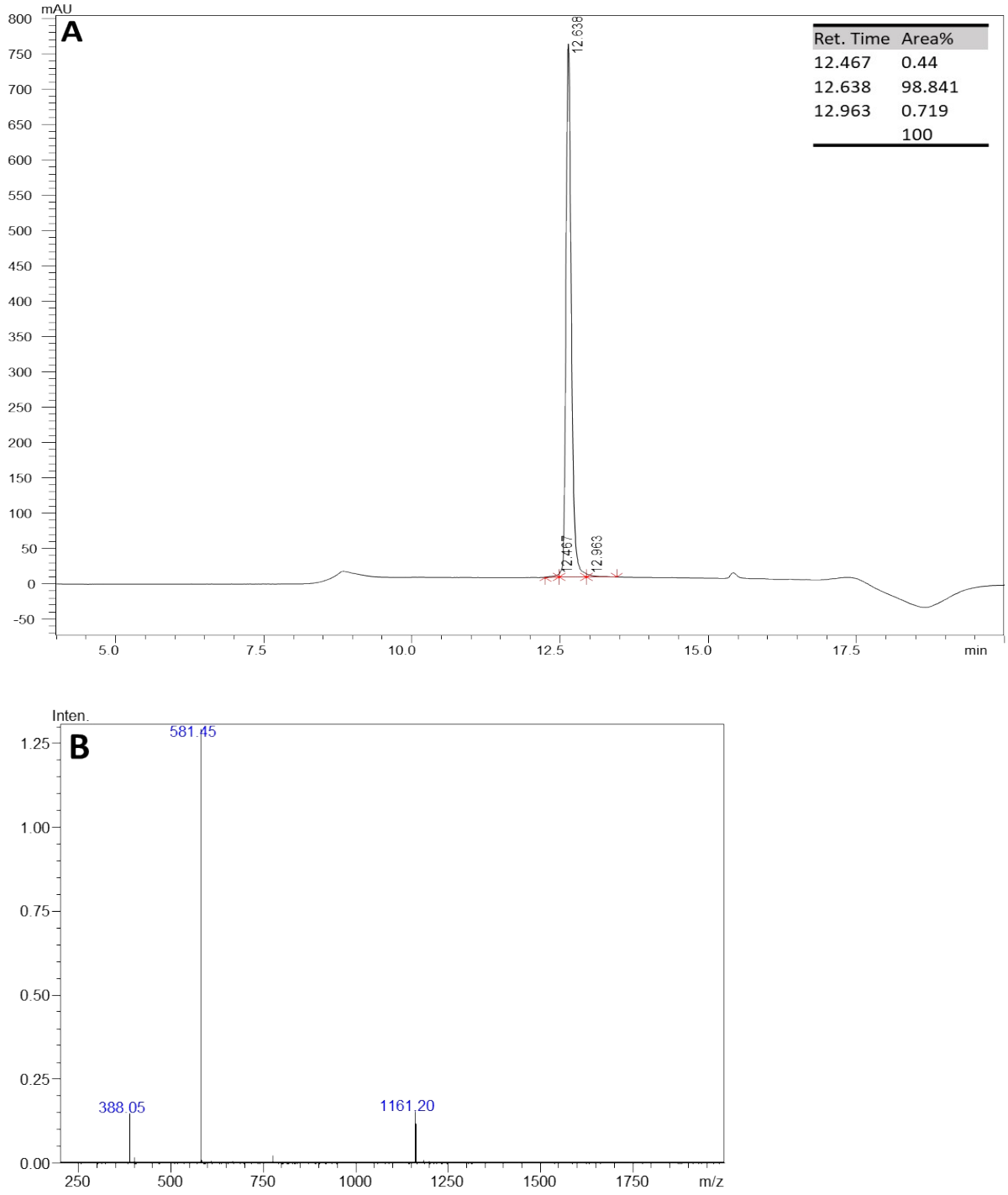

Figure S11. LC-MS profile for [Ala^9]-Polymyxin B$_3$. (**A**) LC profile at 214 nm. (**B**) MS spectrum of the peak at 12.638 min.

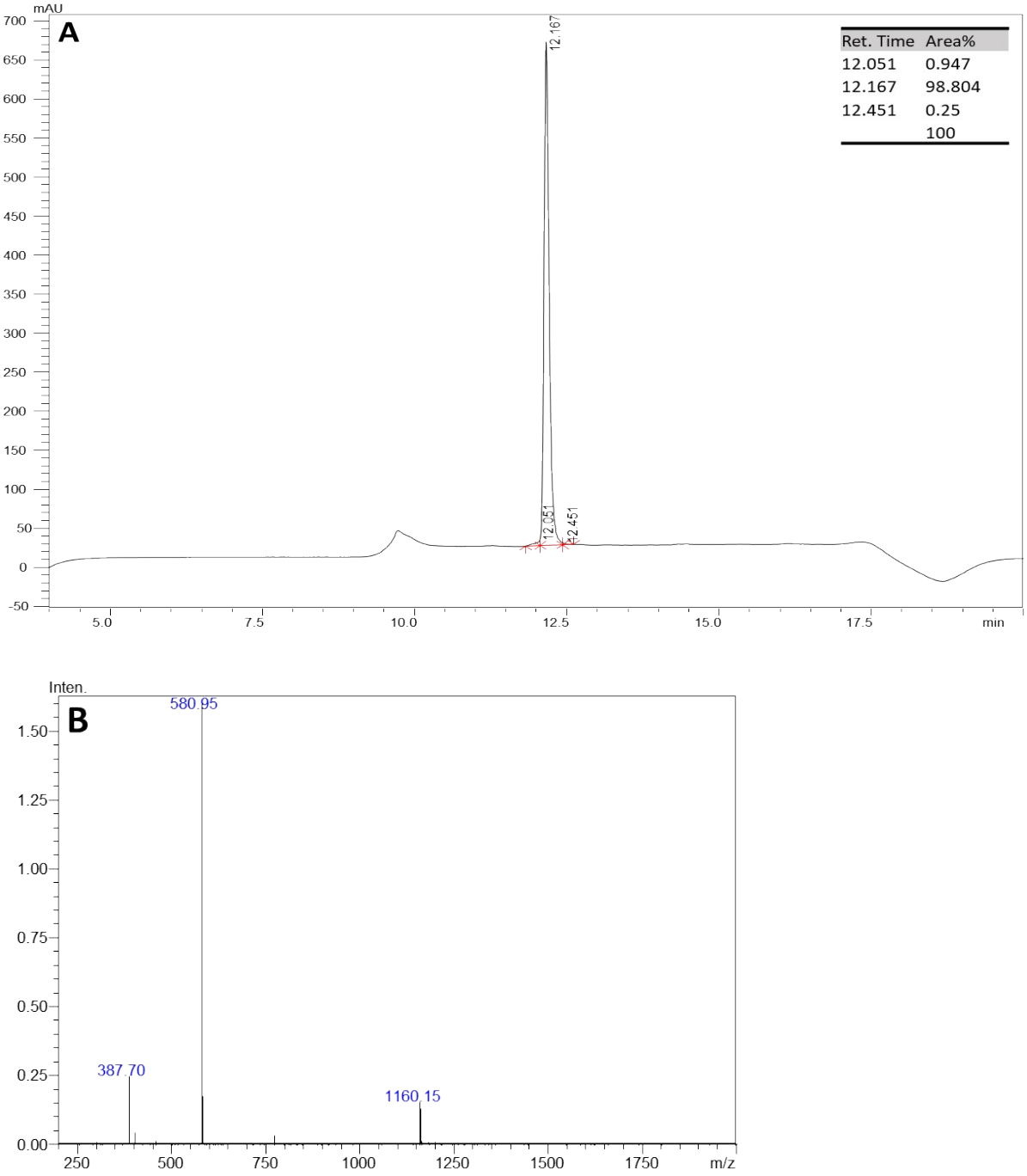

Figure S12. LC-MS profile for [Ala^{10}]-Polymyxin B$_3$. (**A**) LC profile at 214 nm. (**B**) MS spectrum of the peak at 12.167 min.

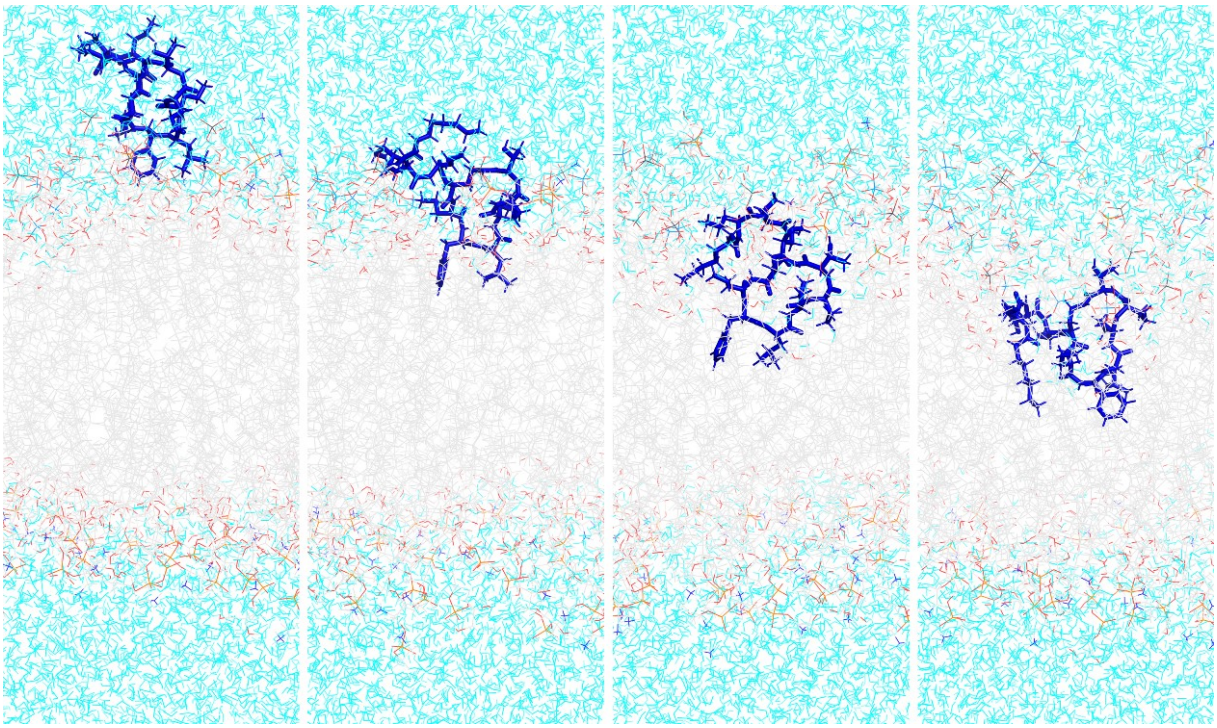

Figure S13. Snapshots of the penetration of polymyxin B_3 into the *A. baumannii* outer membrane. The polymyxin molecule is shown in blue sticks, water molecules are shown in cyan lines, and the head groups and hydrocarbon tails of the outer membrane are shown in red and gray lines, respectively.

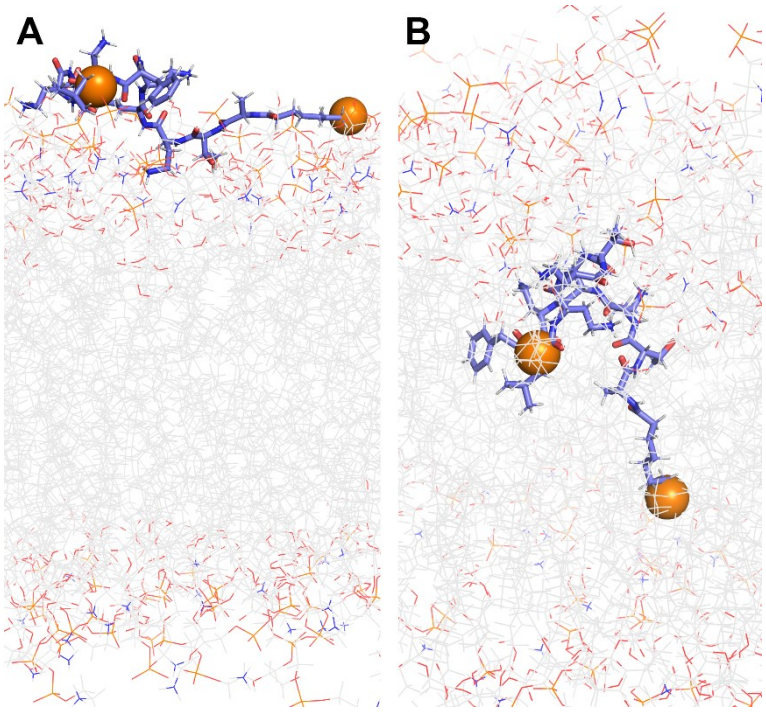

Figure S14. Conformations of [Ala^1]-PMB$_3$ in the (A) head group region and (B) hydrophobic center of the outer membrane.

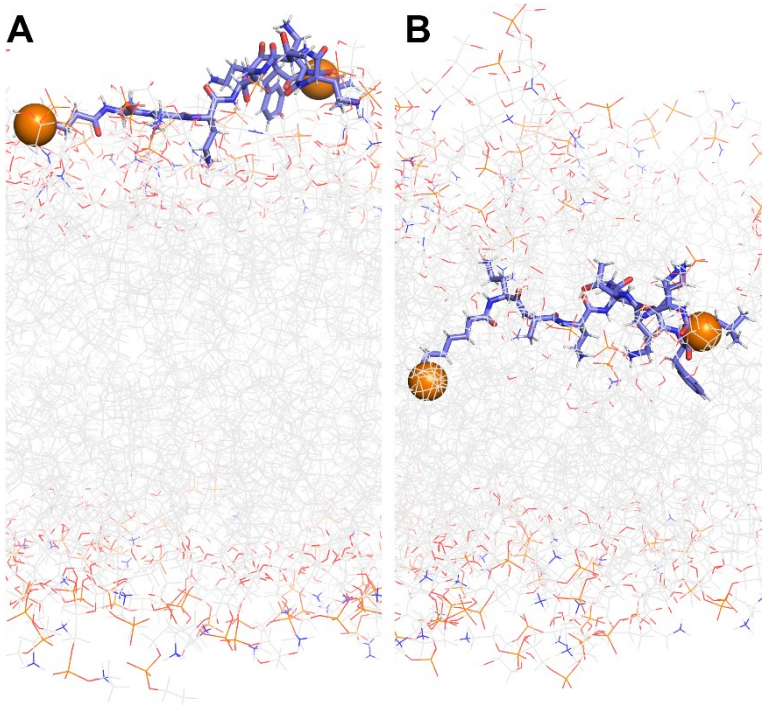

Figure S15. Conformations of [Ala^2]-PMB$_3$ in the (A) head group region and (B) hydrophobic center of the outer membrane.

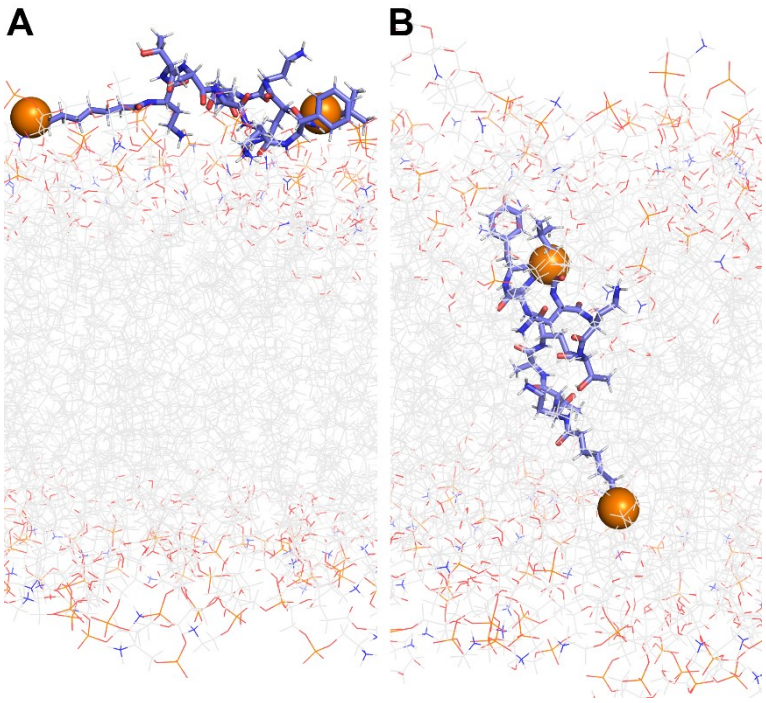

Figure S16. Conformations of [Ala^3]-PMB$_3$ in the (A) head group region and (B) hydrophobic center of the outer membrane.

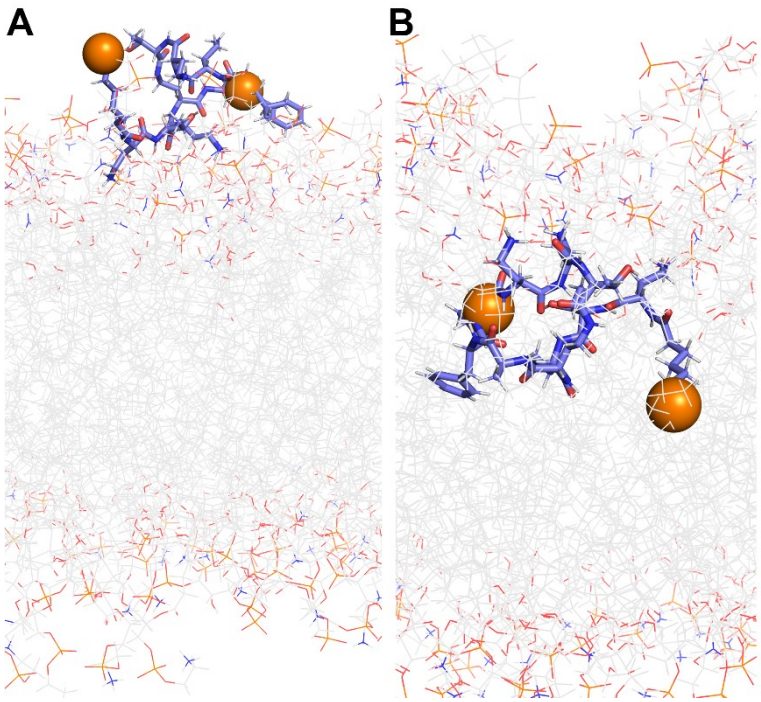

Figure S17. Conformations of [Ala^5]-PMB$_3$ in the (A) head group region and (B) hydrophobic center of the outer membrane.

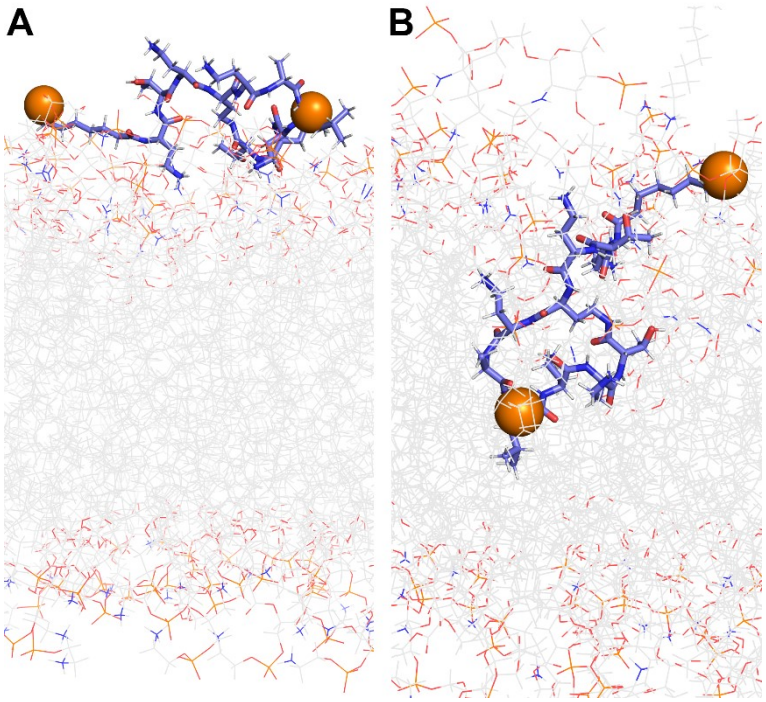

Figure S18. Conformations of [Ala^6]-PMB$_3$ in the (A) head group region and (B) hydrophobic center of the outer membrane.

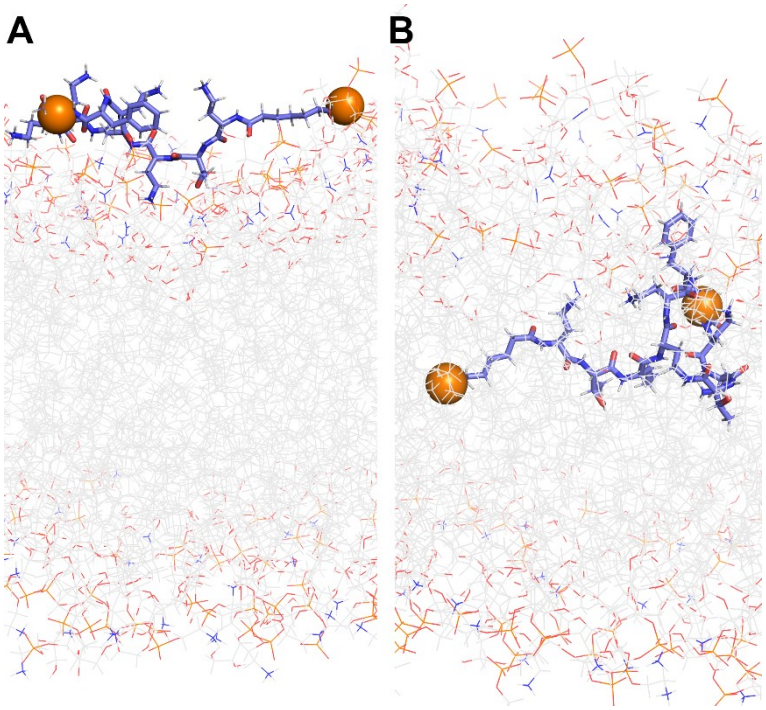

Figure S19. Conformations of [Ala^7]-PMB$_3$ in the (A) head group region and (B) hydrophobic center of the outer membrane.

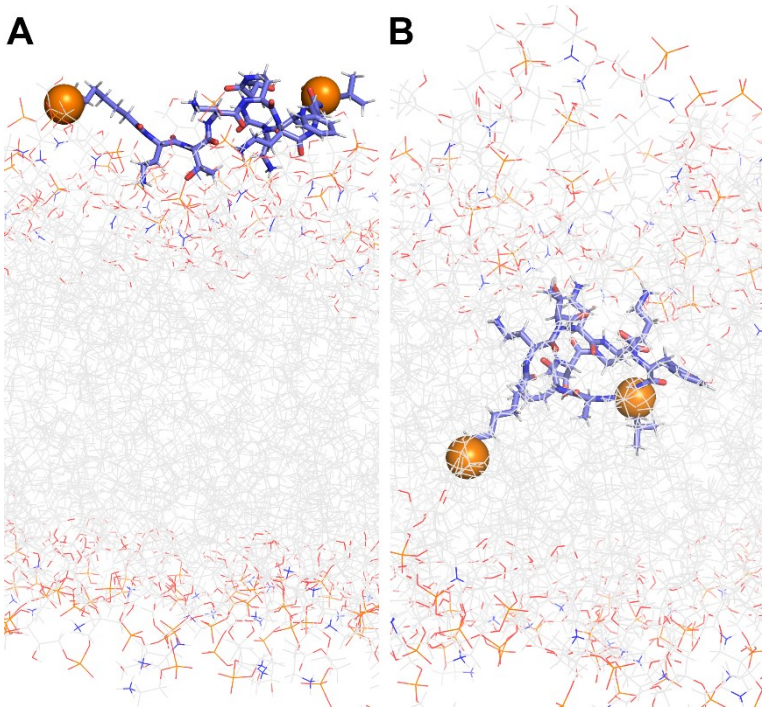

Figure S20. Conformations of [Ala^{8}]-PMB$_3$ in the (A) head group region and (B) hydrophobic center of the outer membrane.

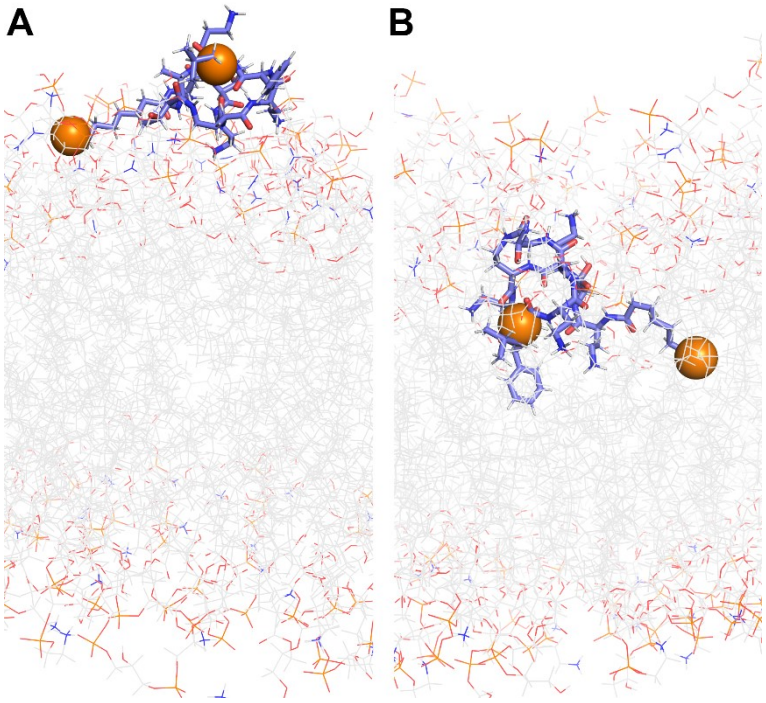

Figure S21. Conformations of [Ala^{9}]-PMB$_3$ in the (A) head group region and (B) hydrophobic center of the outer membrane.

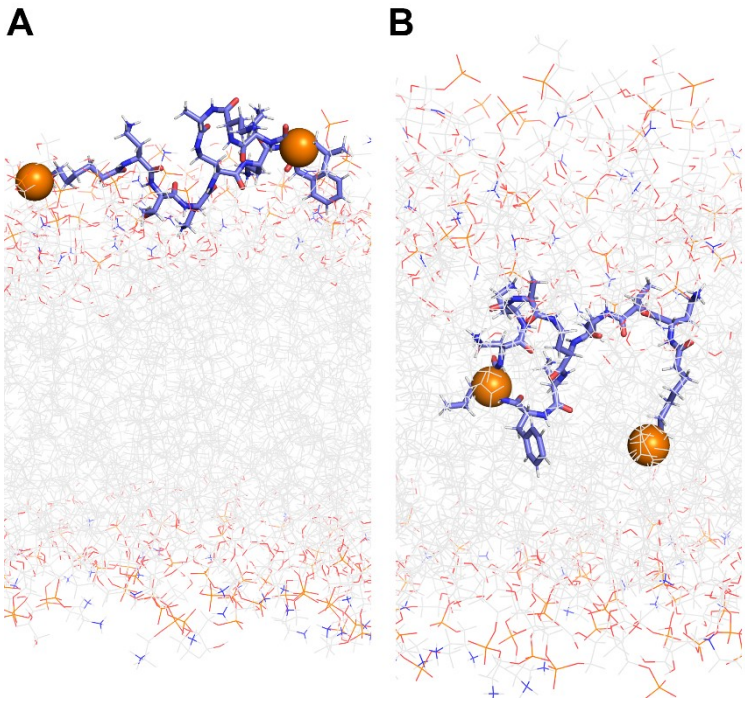

Figure S22. Conformations of [Ala^{10}]-PMB$_3$ in the (A) head group region and (B) hydrophobic center of the outer membrane.

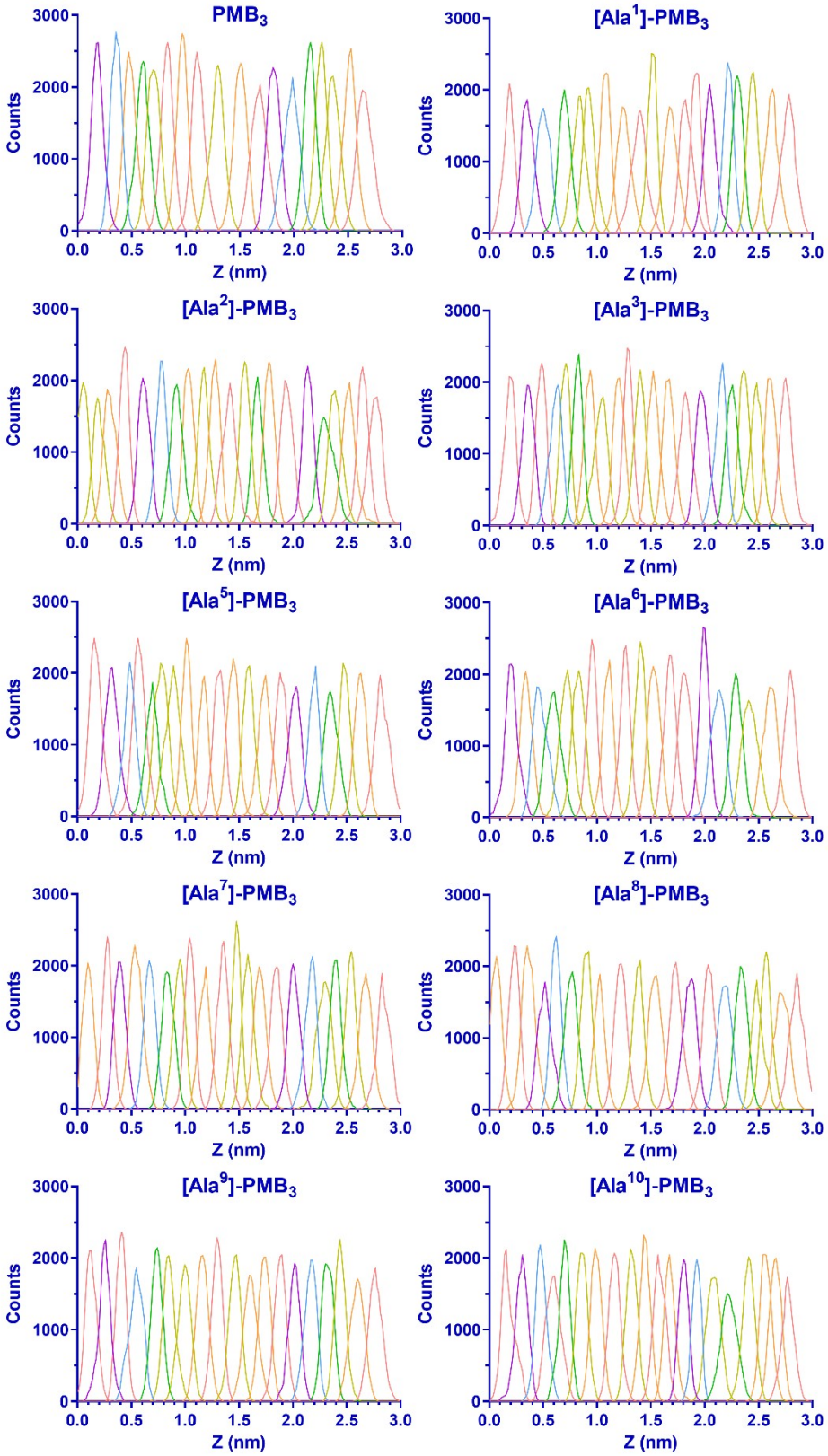

Figure S23. Umbrella sampling of polymyxins during the molecular simulations.

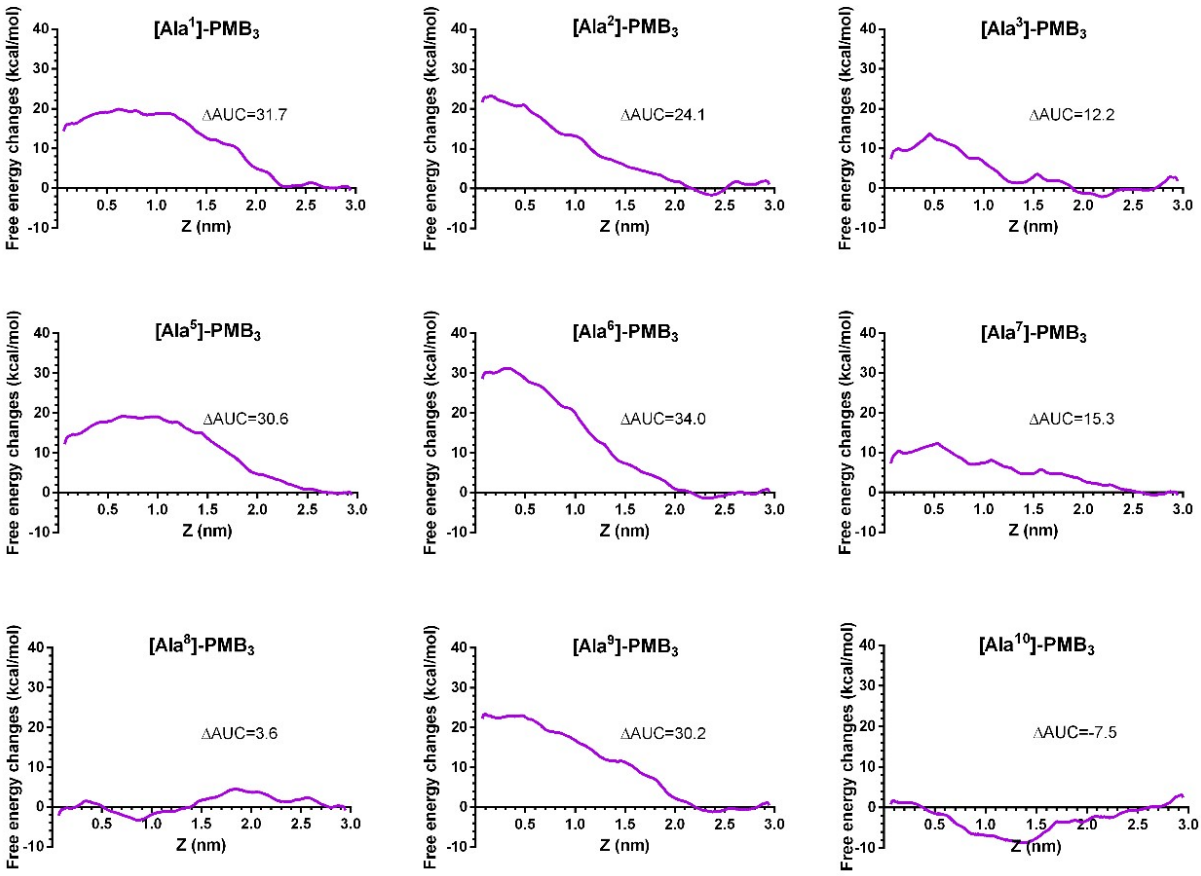

Figure S24. Free energy changes of polymyxin analogs compared to polymyxin B_3. ΔAUC is the difference in free energy between polymyxin B_3 and its alanine-substituted analogs.

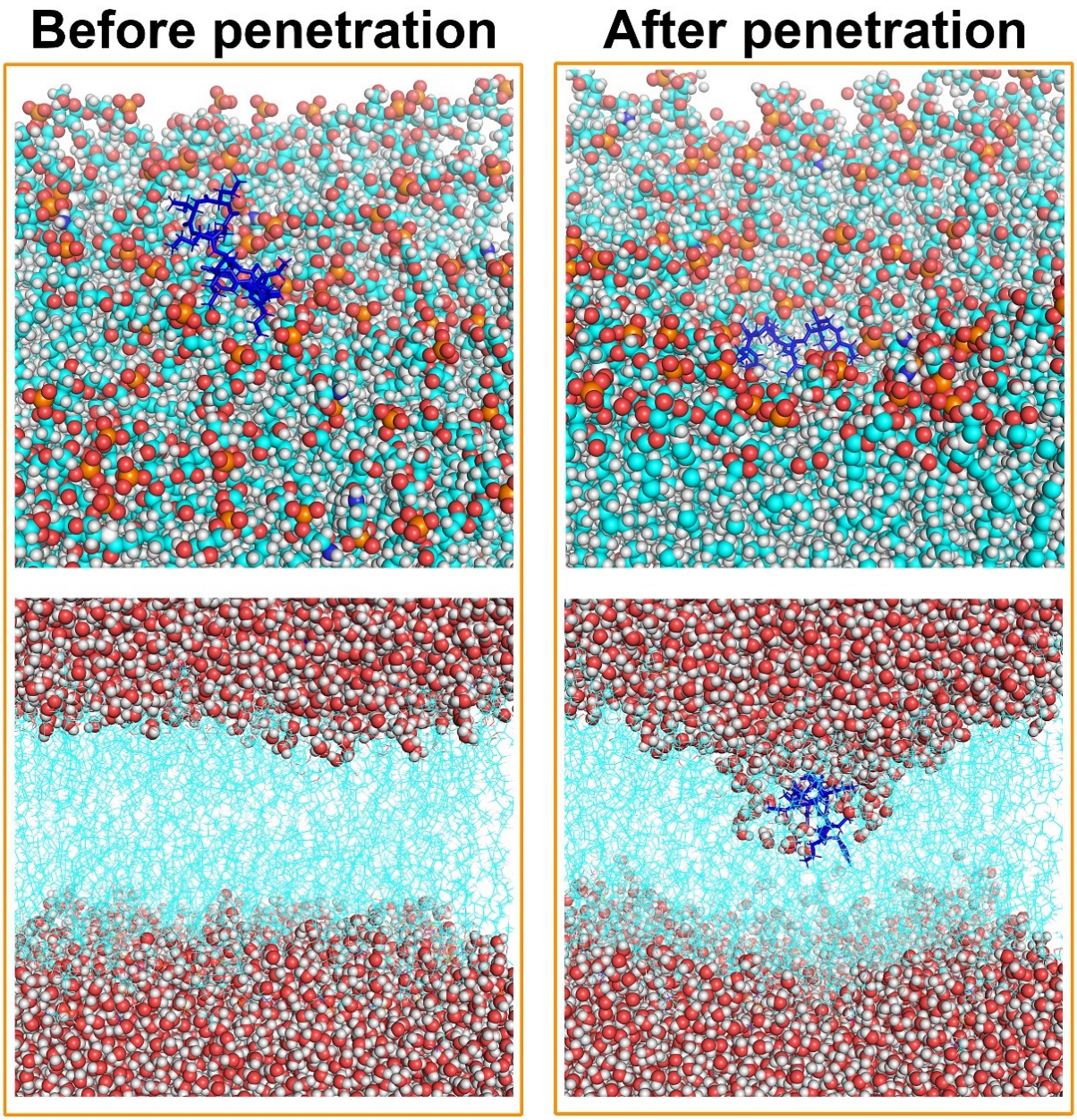

Figure S25. Disorganization of the *A. baumannii* outer membrane caused by the penetration of polymyxin B_3. The upper and lower panels show the top and side views, respectively. The polymyxin molecule is shown in blue sticks, water molecules are shown in spheres with red oxygen atoms and white hydrogen atoms. The outer membrane is shown in cyan lines.

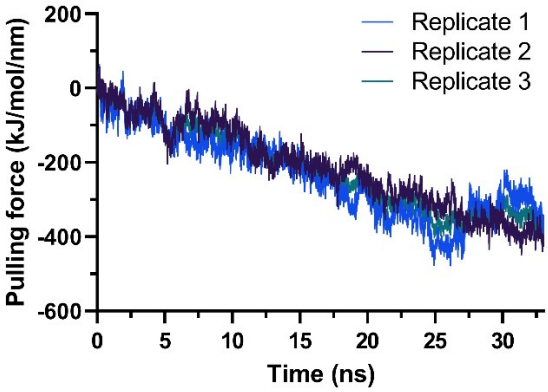

Figure S26. Pulling force profiles of polymyxin B_3 from three independent steered simulations.

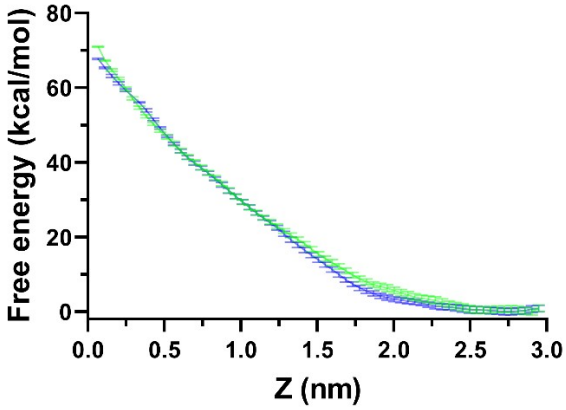

Figure S27. Free energy profiles of polymyxin B_3 penetrating into the outer membrane. The profiles were calculated based on the umbrella sampling simulations with each simulation window of 50 ns (green) and 200 ns (blue).

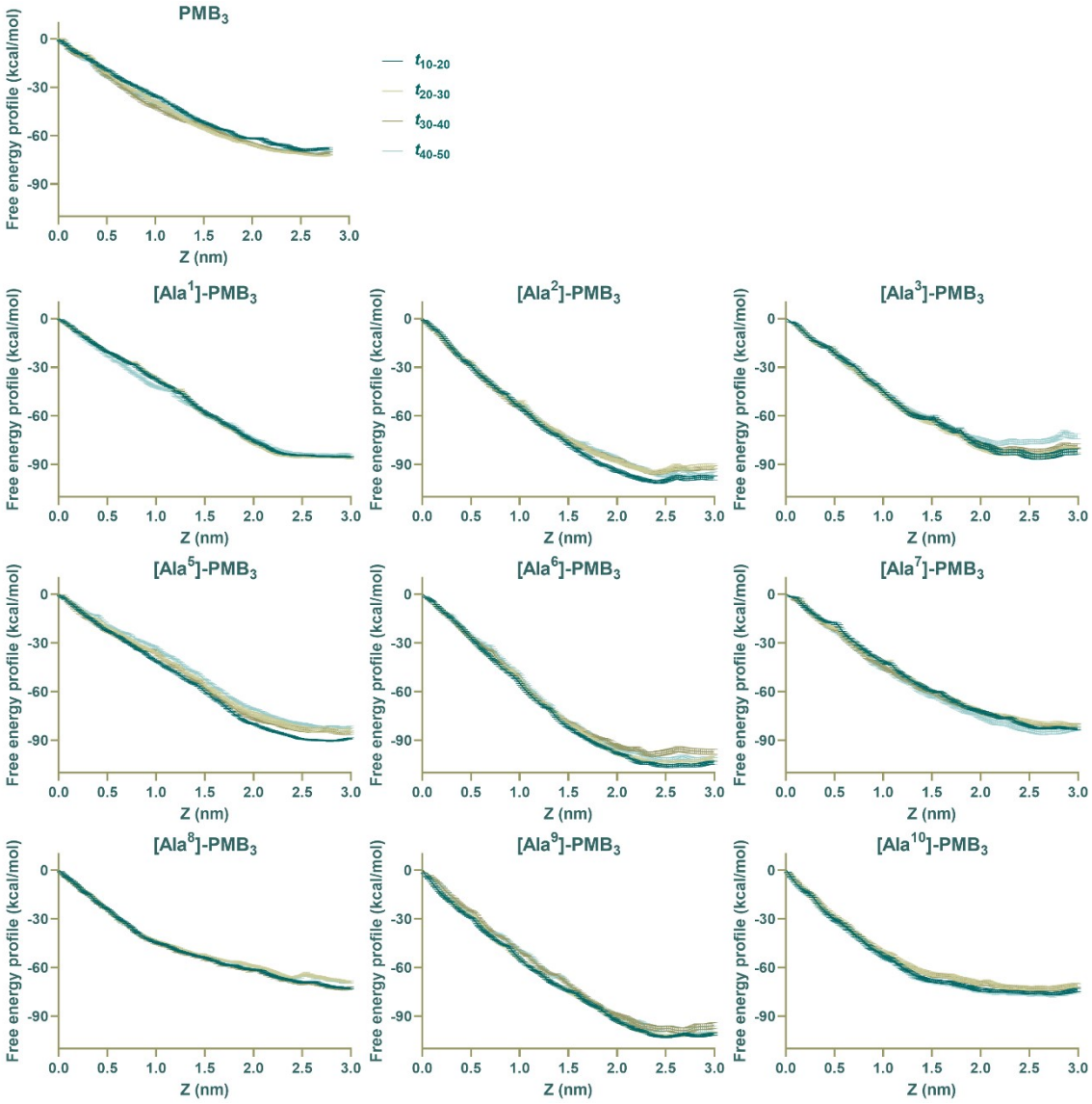

Figure S28. Free energy profiles of polymyxin analogs calculated from 10-ns time blocks.

The free energy profiles from four time-blocks show the simulation convergence.

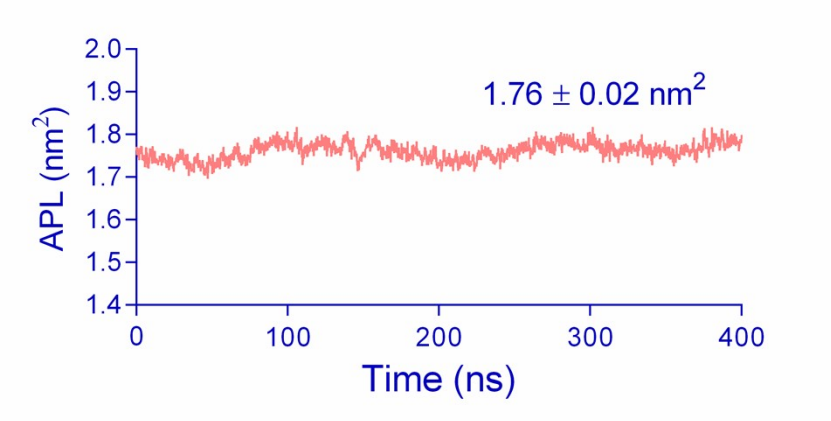

Figure S29. Area per lipid A molecule calculated from 400-ns nonrestraint simulations. The minor fluctuations indicate that the outer membrane system reached the equilibration state.